Cylinder Thermal State Detection from Pressure Cycle in SI Engine

I. Arsie - G. Flauti - C. Pianese - G. Rizzo
Dipartimento di Ingegneria Meccanica - Università di Salerno
84084 Fisciano (Sa) - Italy
ph: +39.089.96.4069 - fax: +39.089.96.4037
e-mail: grizzo@unisa.it
Web page: http://www.tecno.diiie.unisa.it/dimec/macchine

ABSTRACT

In this paper the problem of engine thermal state detection is approached by means of measured in-cylinder pressure cycle analysis for SI engine. The proposed procedure could overcome the difficulties related with the direct cylinder wall temperature measurement which is fundamental for engine control application and cycle modeling, due to its influence on engine heat flow, emissions and friction losses.

The proposed technique is based on the treatment of measured in-cylinder pressure cycle which brings in itself most of the information concerning heat flow, engine operation and emission formation processes. The developed methodology relies on the identification of the instantaneous polytropic compression coefficient as function of crank angle and pressure data in order to estimate the occurrence of an adiabatic condition between cylinder wall and engine gas mixture during compression stroke. The crank angle position where the detected polytropic coefficient approaches the value corresponding to the local adiabatic one is assumed as the inversion point for the net heat flux between cylinder wall and gas mixture. Under steady-state heat flow condition it is customary to accept that both gas mixture temperature and cylinder wall temperature are the same at the occurrence of the detected adiabatic condition. Therefore, the mean gas mixture temperature is computed from a simple thermodynamic relationship as function of pressure, volume displacement and polytropic coefficient.

The technique is explained in detail, also discussing the influence of measurement errors and the computed wall temperature profiles for a large set of experimental data during steady-state engine operating condition. A preliminary numerical analysis has been conducted by modeling unsteady heat flow between cylinder wall surface, thermal boundary layer and mixture gas in order to evaluate the accuracy of the steady-state hypothesis assumed for the proposed technique.

Key-words: Engine, Cylinder Wall Temperature, Engine Control

INTRODUCTION

The evaluation of engine thermal field is a significant objective for both internal combustion engine modeling and control design due to its strong influence on engine heat flow and engine performance (e.g. fuel consumption, emission levels, mechanical losses).

In the field of electronic control for spark ignition engines the cylinder wall temperature represents one of the critical parameters and plays a key role for the definition of transient control strategies. Nowadays, the engine coolant water temperature is taken into account for control purposes, though it exhibits inadequate dynamic signal features due to the high thermal inertia related with the heat exchange process between gas mixture, chamber wall and coolant fluid. Thus, direct information of engine in-cylinder wall thermal state would be beneficial for most engine control problems and constitutes an essential information for thermal heat transfer computations in engine models as well. The direct measurement of the cylinder wall thermal field by classical experimental techniques seems not suitable for on-line applications on production engines, due to costs and measurement difficulties involved.

Since many decades, researchers have developed several techniques based on pressure cycle measurement, oriented to optimum spark control, knock control, air-fuel ratio control, charge temperature estimation and misfire detection [1]. The authors themselves have already approached a technique, originally proposed by Gassenfeit, Powell and Patrick [2], for air-fuel ratio estimation based on measured pressure cycle statistical moments [3], [4].

Actually, limited application of PBC (Pressure Based Control) techniques can be observed due to the high cost of the pressure sensors. Nevertheless, this approach would allow to obtain all the required information from one measurement, thus compensating for the higher effort required [6].

The proposed methodology is based on the steady-state heat transfer theory which states that the adiabatic heat flow condition is reached when zero temperature gradient occurs. As it will be explained in the following, this condition is detected by means of thermodynamic polytropic process modeling. A preliminary analysis, mainly devoted to test the proposed approach has been described in previous

works [4], [5]. The results obtained from a direct use of this methodology, for both steady state and transient engine operating conditions, have shown the potentiality for engine thermal state detection application. Thus, further analyses have been conducted in order to assess the technique with respect to the measurement errors induced by sensor resolution and to the approximation of a steady-state heat transfer model.

In the following the technique adopted for the estimation of the mean combustion chamber wall temperature is described and the most relevant results are presented.

CYLINDER WALL TEMPERATURE EFFECTS

The cylinder wall temperature is a meaningful information on the engine thermal state, and earlier studies showed that it influences remarkably the engine heat transfer and the exhaust emissions [7].

Except than in early stages of cold starts, at the beginning of the compression stroke the chamber surface mean temperature is greater than the gas temperature. As the compression proceeds the gas temperature increases and the heat flux between the cylinder walls and the gas core region, across the thermal boundary layer, is inverted, as result of the compression work exerted on the gas by the piston. The influence of cylinder wall temperature variations on the surface heat transfer during the combustion process can be neglected, due to the relatively high temperature of burned gases, while it is more significant during intake and compression strokes when the gas temperature is lower. In these conditions a reduction in the wall temperature would cause a decrease in the surface heat transfer and in the bulk temperature of the unburned gases prior to combustion, and consequently a reduction in the temperature of the burned gases.

The in-cylinder wall temperature has also a strong influence on the exhaust emissions, particularly HC and NOx. For HC, two of the main sources of formation, such as the fuel absorption in the oil layer and the crevice volume, reduce dramatically as the chamber surface temperature increases [8]. The former due to a reduction in the oil layer thickness which is directly related to the wall temperature, the latter because variations on cylinder and piston temperatures produce changes in their thermal dilatation and consequently in the top-land volume, thus changing the amount of fuel trapped within this region.

Unlike the HC, the NOx emissions increase substantially with the wall temperature. This effect can be explained considering that wall temperature influences the maximum temperature in the core region, by means of its effects on the thermal flow at the beginning of the compression. The NOx exhaust emissions are primarily driven by chemical kinetics mechanisms which are non linearly dependent to the highest temperature reached in the cycle, thus even a slight increase in the peak temperature produces a large increase in emissions [9].

CYLINDER WALL TEMPERATURE ESTIMATION

The proposed procedure allows to evaluate the characteristic in-cylinder gas temperature during compression stroke which is assumed as a reference mean combustion chamber wall temperature. The technique is derived from thermodynamic considerations, assuming that during the compression stroke the in-cylinder mixture experiences a process with a heat flux between gas and cylinder wall. Except than in early stages in cold starts, during the first stages of the compression the net heat flux is directed from the wall to the gas (the wall temperature is greater than gas temperature), while as the compression advances the inversion of the heat flux takes place (the gas temperature reaches levels higher than the wall temperature). Starting from these considerations, it is customary to postulate the occurrence of an adiabatic condition (i.e. zero net heat flux between gas and wall) during the compression stroke. The compression process can be described with a polytropic relationship with variable exponent as function of crank angle:

$$pV^{m(q)}=\text{const} \qquad (1)$$

Neglecting the effects of the entropy production due to irreversibility and to gas friction, the adiabatic condition can be found in correspondence of the crank angle where the exponent $m(q)$ reaches the instantaneous value of the specific heat ratio $\boldsymbol{k=c_p/c_v}$ (i.e. the exponent of the adiabatic isoentropic process). If it is assumed that the adiabatic condition represents a thermal state where the temperature gradient between the wall surface and the gas is zero, it follows that in this condition the gas temperature is equal to the average cylinder wall temperature.

Nevertheless the above considerations are valid under the hypothesis of a steady-state heat transfer process, while more detailed analyses have shown that the time at which a thermal flux can be neglected is not necessarily the same at which a zero temperature gradient is reached. This is due to a time lag between cause (temperature gradient) and effect (thermal flux) [9], [10], [11], [12], [13], [14].

A further unsteady process has to be considered concerning with the surface temperature cyclic variation, which have been analyzed by means of theoretical studies on heat transfer within an infinite slab [10], [11], [15]. These studies have evidenced that the thickness of the penetration layer within the wall where the unsteady thermal field occurs is limited to few millimeters. Moreover surface temperature fluctuations are locally relatively small (i.e 5-10 K)

enforcing the hypothesis to assume a constant surface temperature over an engine cycle [10], [11], [15].

It must be also pointed out that in a combustion chamber a complex thermal field takes place, with significant spatial distribution as well as cyclic time fluctuations. In particular, the "effective" wall temperature tends to increase as compression phase proceeds, due to the increasing influence played by the regions closer to the TDC, where the wall temperature is higher.

At the present stage of this work, neither the surface temperature cyclic variation nor dynamic effects due to boundary layer have been considered, because of the computational constraints imposed by an on-board real-time estimation. Therefore, the proposed technique allows to determine an index representative of the thermal state rather than an exact knowledge of the wall temperature distribution. To derive the gas mixture temperature at the identified inversion heat flux crank angle the gas law is used, starting from the knowledge of pressure, volume, air fuel ratio, residual fraction and gas temperature at IVC. Classical gas property routines have been used for these calculations [10].

Applying equation (1) between two generic crank angle positions q-Dq and q+Dq, the value of the polytropic exponent is given by:

$$m(q) = \frac{\log\left(\frac{p(q+\Delta q)}{p(q-\Delta q)}\right)}{\log\left(\frac{V(q-\Delta q)}{V(q+\Delta q)}\right)} \qquad (2)$$

The desired local value of polytropic exponent $m(q)$ could be in principle computed for each crank angle (2), referring to a small Dq (e.g. Dq = 1 ÷ 5 [deg]). Nevertheless, the measurement error, due to the influence of transducer resolution and to measurement noise, can significantly affect the resulting value of the polytropic exponent, particularly for small Dq. This effect is remarked in Figure 1, where adiabatic and polytropic index, computed from measured pressure data, are plotted vs. crank angle[1] for Dq = 1 [deg]. In the figure, the different trends of the polytropic index are due to the fact that pressure values are not continuous but assume discrete values, according to sensor resolution (0.05 [bar] in the actual case). Therefore, a zero polytropic index is computed when the pressure increment is lower than sensor resolution (i.e. up to -105 [deg]), while over estimation and under estimation occur when this value or its multiples are detected (i.e. 0.05, 0.10 [bar], etc…). However, this problem can be overcome making use of classic filtering techniques which allow to reduce the discretization effects in order to obtain an univocal trend of the polytropic index along the compression stroke. Furthermore, a strong influence on polytropic index estimation is exerted by the reference pressure at the BDC, which is commonly referred to the mean manifold pressure. A parametric study has been conducted showing that even small error in setting initial pressure value (i.e. about 0.01 [bar]) give rise to strong discrepancies between expected polytropic trends and those derived from eq. 2. This analysis has confirmed the need of estimating the correct absolute BDC pressure value for each cycle. Unfortunately a direct identification of this value by means of classic least square techniques applied to pressure cycle experimental data is unfeasible due to strong correlation between initial pressure and polytropic index trend.

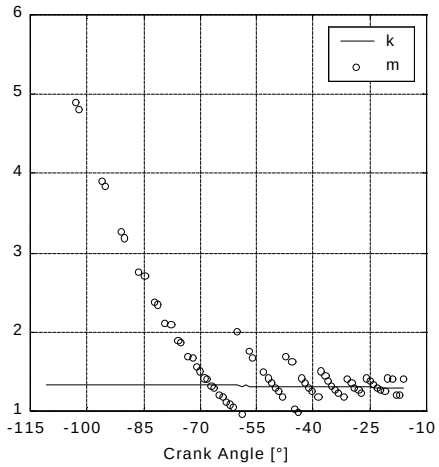

Figure 1 – Comparison between $k(q)$ *and* $m(q)$ computed by eq. 2 making use of measured pressure cycle with Dq = 1 [deg]. (Torque = 50 [Nm], rpm = 2000, AFR = 14.6, Spark adv. = 25 [deg]).

In order to test the technique avoiding the discretization effects deriving from measurement resolution and the uncertainty due to initial pressure value, a detailed analysis has been carried on a set of simulated cycles referred to 157 experimental engine operating condition. The simulated cycles have been computed using a two zone thermodynamic model with a given wall temperature and assuming a Woschni heat transfer model [16]. According to Woschni model assumptions the polytropic index estimated by (eq. 2) presents a linear trend over the whole set of data and the assumed wall temperature is properly reproduced. In Figure 2 the values of polytropic index, computed according to the described procedures are shown for a generic engine condition. It is worth to mention that the range of variation for the polytropic index is in a good agreement with the expected theoretical values [9], while the direct application of eq. 2 resulted in unphysical values as shown above (Figure 1).

[1] Crank angle degree is referred to TDC (i.e. -180 [deg] corresponds to BDC while 0 [deg] is TDC).

Therefore for each engine operating condition the polytropic index has been expressed as linear function of crank angle. The coefficients *a* and *b* have been computed via linear regression from simulated pressure data:

$$m(q) = a \cdot q + b \qquad (3)$$

The coefficients *a* and *b* exhibit a strong correlation (Figure 3) such that *a* can be expressed as function of *b* and engine speed:

$$a = q_1 + q_2 \cdot b + q_3 \cdot \frac{rpm}{1000} \qquad (4)$$

The three coefficients q_1, q_2 and q_3 have been identified with least square technique from the whole set of simulated data.

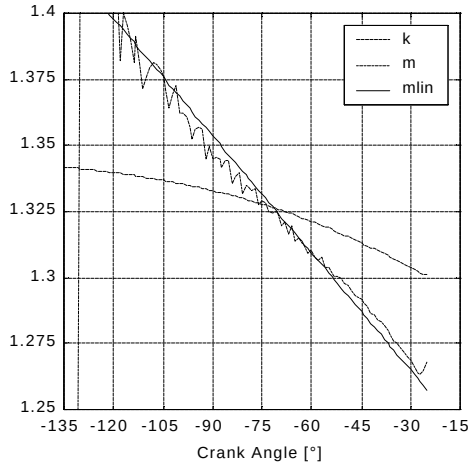

Figure 2 – Comparison between *k(q) and m(q)* computed by eq. 2 making use of simulated data. (Torque = 50 [Nm], rpm = 2000, AFR = 14.6, Spark adv. = 25 [deg]).

The correlation between *a* and *b* (eq. (4)) has been applied for the simultaneous identification of both initial pressure and parameter *b* from measured pressure cycles:

$$\min_{b,p_0} \sqrt{\frac{\sum_{i=1}^{N} (p(i) - p_{lin}(i))^2}{N}} \qquad (5)$$

where p_0 is the initial pressure, *p* is the experimental pressure data, N is the number of sampled data and p_{lin} is computed through the following iterative relation:

$$p_{lin}(i) = p_{lin}(i-1) \cdot \left(\frac{V(i-1)}{V(i)} \right)^{\overline{m}(i)} \qquad (6)$$

where $\overline{m}(i)$ is the mean value between $m(i\text{-}1)$ and $m(i)$ computed by eqs. 3 and 4. In eq. 6 the first value is the initial pressure p_0 to be identified. The polytropic index trend computed starting from the identification results is then used to evaluate the inversion point for the net heat flux between cylinder wall and gas mixture. It is worth to remember that the correlation between *a* and *b* implies the assumption of a steady-state heat transfer model, according to which gas temperature at inversion point corresponds to a reference temperature for the engine thermal state. Within these hypothesis, the heat-transfer coefficient is assumed to be continuous and positive, thus heat transfer flow is zero only for a zero temperature gradient.

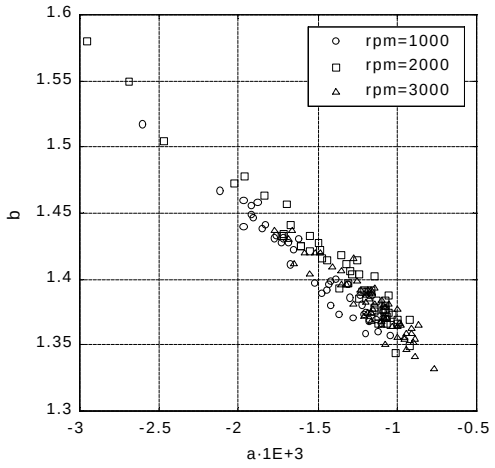

Figure 3 – Correlation between *a* and *b*, R^2=*0.936* (eq. 3).

RESULTS

A set of averaged pressure cycles corresponding to 157 steady-state different operating conditions have been used to assess the developed technique. The experimental tests have been carried at Istituto Motori CNR on a commercial FIAT two liters, four cylinder engine, equipped with multi-point injection system with speed-density electronic control system, also used for the development of other researches whose the present work is part [4], [16]. The engine is mounted on a dynamic test bench, equipped with classical measurement systems, employed for its parametric characterization. The pressure cycle is measured with a Kistler 6001 piezo-electric sensor inserted in one combustion chamber and an AVL Indiskop device is used for sampling and signal conditioning. The mean pressure cycle is obtained from the averaging of 288 sequential pressure time traces. The range of the operating variables for the working conditions is shown in the next table I.

The proposed technique for estimating the reference wall temperature has been applied to the whole experimental data set. At any engine operating condition, the BDC absolute pressure has been identified minimizing eq. 5, and the polytropic trend has been estimated by means of eqs. 3 and 4.

		Lower limit	Upper limit
Engine Speed	[rpm]	1000	3000
Torque	[Nm]	10	90
Spark Advance(*)	[deg]	5	45
Air-Fuel ratio	[/]	11	18
(*) A variable spark advance range has been chosen consistently with correct engine performance to avoid knocking and incomplete combustion.			

table I - Limit values of the engine operating variables for each working condition.

In the figures 4, 5 and 6 the estimated reference temperature, T_w, has been plotted as function of air-fuel ratio and manifold pressure for three engine speed regimes. The plotted surfaces have been derived interpolating the results referred to different spark advance conditions. In these figures the estimated temperature exhibits different behavior depending on engine speed, mainly due to its influence on heat transfer dynamics which has not been modeled at the present stage of work. The influence of engine operating variables on reference wall temperature has been evaluated through a linear correlation analysis and the corresponding indices are reported in tables II-III-IV for different engine speeds.

At lower engine speed (Table II, Figure 4) T_w increases with residual gas fraction (.67)[2], while a remarkable inverse correlation is detected for air mass flow (-.70), and its correlated variables (manifold pressure, torque). Moreover, a slight influence is exerted by spark advance (.19) while an inverse correlation is detected for Air Fuel Ratio (-.31). The residual gas fraction effect can be explained considering that the greater gas charge energy produces an increase in the bulk temperature during compression and consequently enhances the heat transfer towards the wall. Nevertheless, an increase in the air mass flow produces a greater turbulence in the fresh charge and consequently enhances the heat transfer between cylinder wall and gas during induction phase. Such behavior is expected because an increase in turbulence levels promotes gas mixing and energy transport close to cylinder walls leading to a reduction of thermal boundary layer thickness on the combustion chamber surface. On the other hand, at higher engine speed (Table IV, Figure 6), T_w increases with air mass flow (.51); this effect can be explained considering that an increase in the air mass flow, which produces a greater turbulence enhancing the heat transfer, is not able to balance for the greater energy amount due to the combustion of a greater amount of fresh charge. Moreover a weak inverse correlation is detected for residual gas (-.42) due to its relative smaller amount with respect to intake gas charge. It has to be remarked that at high engine speed and low load conditions the inversion section point was detected earlier than inlet valve closing, probably due to a lower wall temperature with respect to gas charge.

In the Figure 7, the mean reference wall temperature is plotted vs. engine speed and engine torque for the whole experimental data set, from which it emerges that the maximum temperature values are reached for higher engine torque and speed, as expected from basic physical consideration. On the other hand, the results presented in a previous paper [5] evidence a different trend with respect to engine load with a reduction of wall temperature as the engine load increases. This behaviour is mainly caused by a different procedure used for the inversion point detection while other effects are related with a rough approximation for the initial pressure evaluation. Nevertheless, the results presented herein are more accurate though an unpredictable effect due to heat transfer dynamics has to be investigated as discussed in the following section.

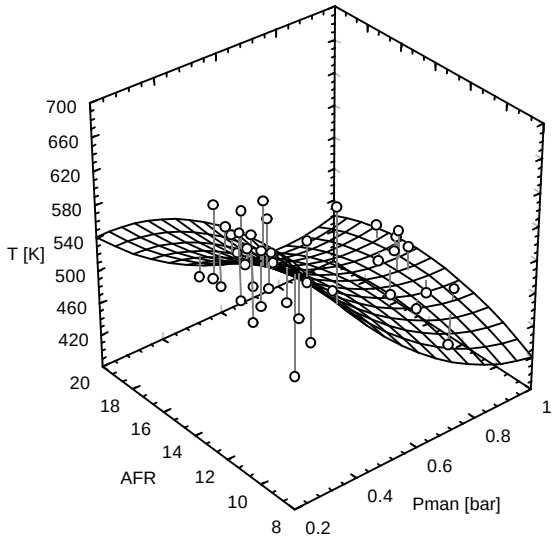

Figure 4: Mean wall temperature as function of manifold pressure and air fuel ratio (Engine speed=1000 [rpm]).

	Sp. Adv.	Man pres	AFR	Torq	Air M.F	T_w	Res. gas
Spark adv.	1.00	-.66	.06	-.56	-.65	**.19**	.70
Manif. pres	-.66	1.00	.16	.98	1.00	**-.69**	-.97
AFR	.06	.16	1.00	.09	.18	**-.31**	-.13
Torque	-.56	.98	.09	1.00	.98	**-.72**	-.95
Air Mass F.	-.65	1.00	.18	.98	1.00	**-.70**	-.97
T_w	**.19**	**-.69**	**-.31**	**-.72**	**-.70**	**1.00**	**.67**
Res. gas	.70	-.97	-.13	-.95	-.97	**.67**	1.00

Table II: Linear correlation indices between operating engine variables for the 43 steady-state engine working condition considered at 3000 [rpm].

[2] The values in brackets are the computed linear correlation index.

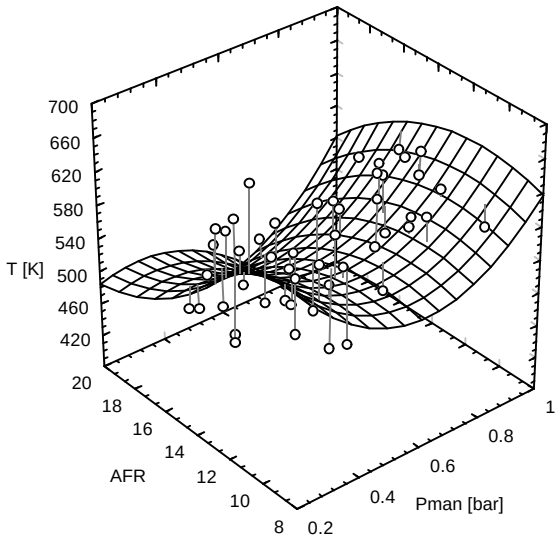

Figure 5: Mean wall temperature as function of manifold pressure and air fuel ratio (Engine speed=2000 [rpm]).

	Sp. Adv.	Man pres	AFR	Torq	Air M.F	T_w	Res. gas
Spark adv.	1.00	-.46	.25	-.33	-.44	**-.68**	.39
Manif. pres	-.46	1.00	-.05	.96	1.00	**.25**	-.95
AFR	.25	-.05	1.00	-.16	.01	**-.44**	.06
Torque	-.33	.96	-.16	1.00	.94	**.24**	-.91
Air Mass F.	-.44	1.00	.01	.94	1.00	**.20**	-.94
T_w	**-.68**	**.25**	**-.44**	**.24**	**.20**	**1.00**	**-.14**
Res. gas	.39	-.95	.06	-.91	-.94	**-.14**	1.00

Table III: Linear correlation indices between operating engine variables for the 53 steady-state engine working condition considered at 2000 [rpm].

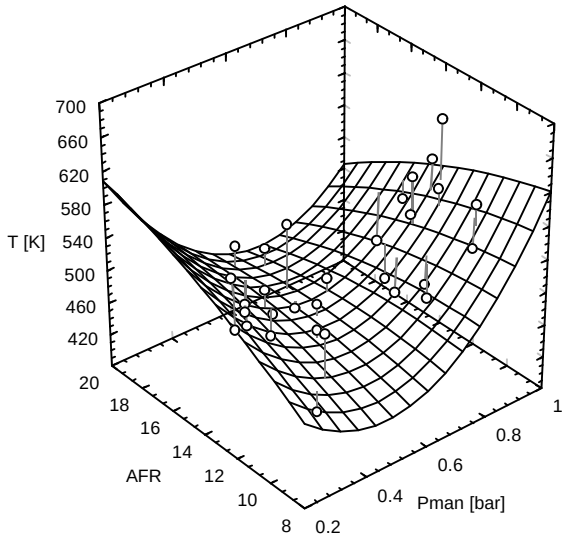

Figure 6: Mean wall temperature as function of manifold pressure and air fuel ratio (Engine speed=3000 [rpm]).

	Sp. Adv.	Man pres	AFR	Torq	Air M.F	T_w	Res. gas
Spark adv.	1.00	-.39	-.07	-.12	-.43	**-.36**	.57
Manif. pres	-.39	1.00	-.14	.94	1.00	**.54**	-.93
AFR	-.07	-.14	1.00	-.31	-.08	**-.22**	.00
Torque	-.12	.94	-.31	1.00	.92	**.46**	-.81
Air Mass F.	-.43	1.00	-.08	.92	1.00	**.51**	-.95
T_w	**-.36**	**.54**	**-.22**	**.46**	**.51**	**1.00**	**-.42**
Res. gas	.57	-.93	.00	-.81	-.95	**-.42**	1.00

Table IV: Linear correlation indices between operating engine variables for the 30 steady-state engine working condition considered at 3000 [rpm].

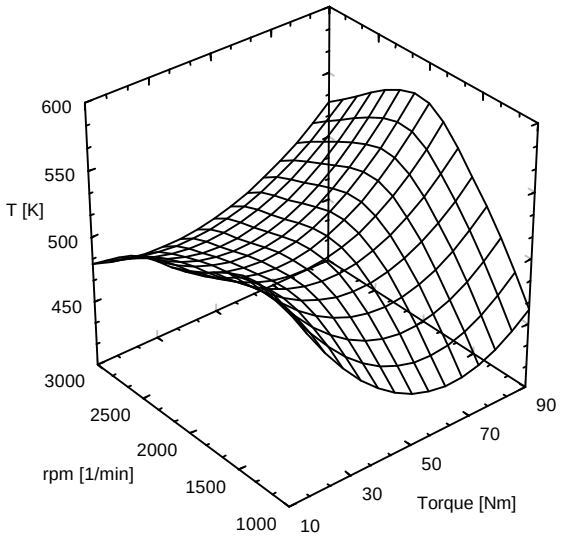

Figure 7 - Mean wall temperature as function of torque and engine speed.

HEAT TRANSFER DYNAMICS

In order to take into account the effects of heat transfer dynamics and the time lag between thermal flux and temperature gradient, a boundary layer model is actually being developed. The model has been designed following the energy balance equation applied to a control volume close to the cylinder wall surface, neglecting the internal energy sources and the mean fluid motion normal to cylinder wall, and assuming one-dimensional heat transfer processes in the normal direction with respect to cylinder surfaces [12], [13] :

$$r \cdot c_p \frac{\partial T}{\partial t} = \frac{dp}{dt} + \frac{\partial}{\partial x}\left[\left(k + k_T\right) \frac{\partial T}{\partial x} \right] \quad (7)$$

where x is the upward normal coordinate while k and k_T are the thermal conductivity and the turbulent eddy thermal conductivity respectively. This latter has been introduced in order to simplify the term accounting for turbulent convection motion and is function of the

temperature T and the normal coordinate x. The energy balance equation has been solved making use of an explicit numerical method [19].

An example of the obtained results is given in Figure 8 where typical simulated temperature profiles are plotted vs. the upward normal coordinate at different CAD and for different wall temperatures.

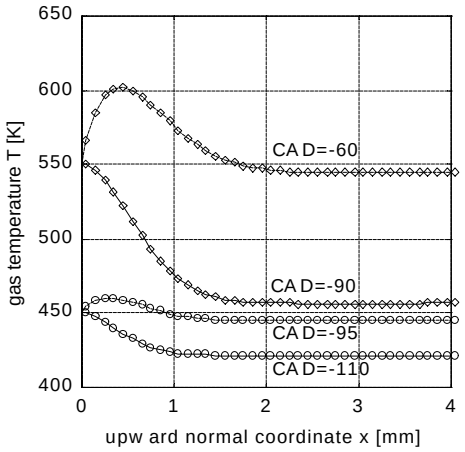

Figure 8 – Comparison between temperature profiles along the upward normal coordinate at two different crank angle positions and for two different wall temperatures. (Torque = 50 [Nm], rpm = 2000, AFR = 14.6, Spark adv. = 25 [deg]).

Depending on wall temperature (T_w = 450÷550 °C), the figure evidences a 15 or 30 CAD lag between the time at which a zero heat flux is reached on cylinder wall (CAD = -110 or CAD = -90) and the time when the gas bulk temperature approaches the wall temperature (CAD = -95 or CAD = -60), thus confirming that dynamic effects exert a strong influence on engine thermal state estimations. More over these results demonstrate that the time lag depends on both engine operating conditions (in particular engine speed) and wall temperature itself.

Further work is needed to establish a procedure to account for the heat flow dynamics effects to be used for engine thermal state detection from pressure cycle measurements.

CONCLUSIONS

A technique for the estimation of cylinder wall temperature, based on the measured pressure cycle for a spark ignition engine, has been described and applied on a large set of engine steady-state operating condition. The feasibility of deriving the engine thermal state reference temperature from pressure cycle has been verified by means of a comparative analysis on simulated and measured engine data. A detailed study has been performed in order to verify the influence of BDC absolute pressure and measured data resolution on the estimated polytropic index. A linear correlation has been derived in order to hold up a least square technique for initial pressure and polytropic index identification.

The development of a boundary layer model is in progress in order to take into account the time phase between thermal flux and temperature gradient within bulk gas and cylinder wall, thus replacing the assumption based on the steady-state model approach. Moreover, the boundary layer model will be assessed making use of motored engine cycle in order to avoid the combustion effects and to estimate more accurately temperature distribution near cylinder walls.

Further studies are in progress to reach a more complete assessment of the technique and to integrate it within advanced pressure cycle based engine control systems, together with the development of other engine variables detection techniques from pressure data.

ACKNOWLEDGMENTS

The financial and technical support of Engine Control Division of Magneti Marelli to the present work is gratefully acknowledged. Part of these research activities have been supported by CNR (96.00042).

REFERENCES

[1] Powell J. D., Engine Control Using Cylinder Pressure: Past, Present and Future, Journal of Dyn. Systems, Meas. and Control, vol. 115, pp. 343-350, 1993.

[2] Gassenfeit E. H., Powell J. D., Algorithms for Air-Fuel Ratio Estimation Using Internal Combustion Engine Cylinder Pressure, SAE Paper 890300, 1989.

[3] Arsie I., Gambino M., Pianese C., Polichetti C., Rizzo G., Estimation of Air-Fuel Ratio from Cylinder Pressure Data in a Spark Ignition Engine for Automotive Applications, 3rd Int. Conference on «High-Tech Engines and Cars», Modena (I), May 22-23, 1997.

[4] Arsie I., Pianese C. Rizzo G., Estimation of Air-fuel Ratio and Cylinder Wall Temperature from Pressure Cycle in S.I. Automotives Engines, IFAC Workshop on Advances in Automotive Control, Mohican State Park, Ohio, USA, February 26 - March 1, 1998.

[5] Arsie I., Flauti G., Pianese C. Rizzo G., Cylinder Wall Temperature Estimation from Pressure Cycle in Spark Ignition Engines, Proc. of 2nd International Conference on "Control and Diagnostic in Automotive Applications", Genova, october 1-2, 1998.

[6] Kawamura, Shinshi, Sato, Takahaschi, Iryama, MBT Control through Individual Cylinder Pressure, SAE Paper 881779, 1988.

[7] Jennings M. J., Morel T., A Computational Study of Wall Temperature Effects on Engine Heat Transfer, SAE Paper 910459, 1991.

[8] Kaplan J. A., Heywood J. B., Modeling the Spark Ignition Engine Warm-Up Process to Predict Component Temperatures and Hydrocarbon Emissions, Sae Paper 910302, 1991.

[9] Heywood J. B., Internal Combustion Engines Fundamentals, MC Graw Hill., 1988.

[10] Ferguson C. R., Internal Combustion Engines, J.Wiley, 1986.

[11] Eckert E. R. G., Drake Jr Robert M., (1989), Analysis Of Heat And Mass Transfer, Hemisphere Publishing Corporation (ISBN 0-89116-553-3).

[12] Jenkin R. J., James E.H. and Malalasekera W., (1996-II), Thermal Boundary Layer Modeling in "Motored" Spark Ignition Engines, SAE Paper 961965.

[13] Jenkin R. J., James E.H. and Malalasekera W., (1996-I), Modeling near Wall Temperature Gradients in "Motored" Spark Ignition Engines, SAE Paper 960070.

[14] Liu Yong and Reitz Rolf D., (1997), Multidimensional Modeling of Engine Combustion Chamber Surface Temperature, SAE Paper 971593.

[15] Anatone M. and Cipollone R., (1998), A Contribution in Calculting the Thermal Fields in Internal Combustion Engines Components, SAE Paper 961127.

[16] Arsie I., Pianese C., Rizzo G., Models for the Prediction of Performance an Emissions in a S.I. Engine - A Sequentially Structured Approach, SAE Paper 980779, in SP-1330, pp. 59-73, "1998 SAE International Congress and Exposition", Detroit, February 23-27, 1998.

[17] Higuma A., Takashi S., Yoshida M., Oguri Y. and Minoyama T., (1999), Improvement of Error in Piezoelectric Pressure Trasducer, Sae Paper 1999-01-0207, in SP-1418.

[18] Rai H.S., Brunt M.F.J. and Loade C.P., (1999), Quantification And Reduction Of Imep Errors Resulting From Pressure Trasducer Thermal Shock in an S.I. Engine, SAE Paper 1999-01-1329, in SP-1446.

[19] Anderson D.A., Tannehill J.C., Pletcher R.H. (1984), Computational Fluid Mechanics and Heat Transfer, Hemisphere Publishing Co.

DEFINITIONS, ACRONYMS, ABBREVIATIONS

LATIN SYMBOLS

AFR	[/] air-fuel ratio
a, b, q_i	regression coefficients
BDC	Bottom Dead Centre
CAD	[deg]crank angle degree
c_p	[KJ/kg K] specific heat capacity
IVC	[deg] inlet valve closing angle
k	[/] specific heat ratio
k	[W/m^2] thermal conductivity
k_T	[W/m^2] turbulent thermal conductivity
m	[/] polytropic relation exponent.
p	[bar] in-cylinder pressure
p_0	[bar] initial pressure
p_{man}	[bar] manifold pressure
R^2	coefficient of determination
rpm	[1/min] engine speed
t	[sec] time
TDC	Top Dead Center
T_w	[K] average cylinder wall temperature
V	[m^3] actual displaced volume
x	[mm] upward normal coordinate

GREEK SYMBOLS

θ	[deg] crank angle position
θ_s	[deg] spark advance
ρ	[kg/m^3] density